Subduction of Decadal North Pacific Temperature Anomalies: Observations and Dynamics

NIKLAS SCHNEIDER AND ARTHUR J. MILLER

Scripps Institution of Oceanography, La Jolla, California

MICHAEL A. ALEXANDER

CIRES, University of Colorado, Boulder, Colorado

CLARA DESER

National Center for Atmospheric Research, Boulder, Colorado

(Manuscript received 9 January 1998, in final form 6 July 1998)

ABSTRACT

Observations of oceanic temperature in the upper 400 m reveal decadal signals that propagate in the thermocline along lines of constant potential vorticity from the ventilation region in the central North Pacific to approximately 18°N in the western Pacific. The propagation path and speed are well described by the geostrophic mean circulation and by a model of the ventilated thermocline. The approximate southward speed of the thermal signal of 7 mm s^{-1} yields a transit time of approximately eight years. The thermal anomalies appear to be forced by perturbations of the mixed layer heat budget in the subduction region of the central North Pacific east of the date line. A warm pulse was generated in the central North Pacific by a series of mild winters from 1973 to 1976 and reached 18°N around 1982. After 1978 a succession of colder winters initiated a cold anomaly in the central North Pacific that propagated along a similar path and with a similar speed as the warm anomaly, then arrived in the western tropical Pacific at 18°N around 1991. Tropical Ekman pumping, rather than further propagation of the midlatitude signal, caused the subsequent spread into the equatorial western Pacific and an increase in amplitude. Historical data show that anomalous sea surface temperature in the equatorial central Pacific is correlated with tropical Ekman pumping while the correlation with thermal anomalies in the North Pacific eight years earlier is not significant. These results indicate no significant coupling in the Pacific of Northern Hemisphere midlatitudes and the equatorial region via advection of thermal anomalies along the oceanic thermocline.

1. Introduction

Several theories have recently been advanced to attempt to explain decadal changes in the North Pacific Ocean. Most of these rely on the long timescale set by baroclinic Rossby wave propagation and its effect on the baroclinic adjustment time of the subtropical oceanic circulation (e.g., Latif and Barnett 1994, 1996; Robertson 1996; Jin 1997; Frankignoul et al. 1997). An intriguing alternative hypothesis is that the tropical and midlatitude ocean are linked by subducted thermal anomalies propagating equatorward along the oceanic thermocline (Gu and Philander 1997; Inui 1997) or in wave guides along the western boundary (Lysne et al. 1997; Venzke 1999). If the ocean can slowly send a signal to the tropical thermocline, which eventually alters tropical sea surface temperature (SST), the atmosphere could rapidly send the signal back to the midlatitudes via teleconnections (Bjerknes 1966; Alexander 1992; Philander 1990) and establish a decadal variation. Because of the short observational record, however, it is difficult to verify such a theory.

Do subsurface ocean observations support the mechanism of subduction as a viable candidate for tropical–extratropical interaction on decadal timescales? Deser et al. (1996, DAT96 hereinafter) presented the first evidence for a subducting temperature anomaly in the North Pacific. With origins north of Hawaii, the peak anomaly appears to move downward (approximately to 200 m) and southward (roughly 8° lat) toward 25°N over a time period 10–15 yr. A great deal of study of the North Pacific thermocline followed that work (e.g., Zhang and Levitus 1997; Inui and Hanawa 1997; Yasuda

Corresponding author address: Dr. Niklas Schneider, Climate Research Division, Scripps Institution of Oceanography 0224, University of California, San Diego, La Jolla, CA 92093-0224.
E-mail: nschneider@ucsd.edu

and Hanawa 1997; Miller et al. 1998; Tourre et al. 1999) and supports the idea of downward and southward moving temperature anomalies in the central North Pacific. But it has not been clearly established if these anomalies reach the equatorial thermocline and what physics controls the excitation, migration, and decay of these anomalies.

Here we address several questions associated with the subduction of temperature anomalies in the North Pacific by studying the available observations (White 1995) in a new way and using simple models to help interpret them. What is the horizontal, vertical, and temporal character of the subducting cold anomalies found by DAT96 in the 1980s? Is that event unique or are there other subducting anomalies in the historical record? Do anomalies move far enough south to interact with the equatorial thermocline? Our novel approach is to analyze the 3D evolution of temperature anomalies in the North Pacific in terms of isotherm depths and potential vorticity (PV). This leads to a clear delineation of decadal anomalies in regions associated with recirculation, ventilation, and shadow zones of the North Pacific (e.g., Luyten et al. 1983, hereinafter LPS83; Talley 1985).

Is the downward and southward migration of these temperature anomalies consistent with the physics of subduction? Anomalous subduction has often been considered as salinity-compensated temperature anomalies being advected by the mean velocity field along mean isopycnals. Liu (1999a,b) has proposed that higher-mode baroclinic waves may also be advected along isopycnals. These anomalies would not be salinity compensated but would have an anomalous pressure and velocity signature. Local forcing by Ekman pumping could also explain temperature anomalies in the mid-ocean if wind stress curl has decadal variations (e.g., Trenberth 1991; Miller et al. 1998). Baroclinic wave propagation on interannual timescales may obscure the subducting temperature anomalies (Miller et al. 1997), and may explain why the DAT96 anomalies were found to increase with time and depth. We study the motion of the subducting anomalies by invoking the ventilated thermocline theory of LPS83 to clarify the roles of subduction and wind forcing. Do the anomalies follow a path along constant PV according to this theoretical framework?

What processes drive these subducting anomalies? The past several decades have seen evidence for regime shifts in both the midlatitudes (Trenberth 1990; Graham 1994; Miller et al. 1994a; Mantua et al. 1997) and the Tropics (Kleeman et al. 1996; Latif et al. 1997; Goddard and Graham 1997). Are these regime changes associated with the surface forcing in the North Pacific that in turn drives the subducting anomalies? Is the surface forcing primarily diabatic, driving the heat equation, or adiabatic, affecting the vorticity equation (cf. Liu 1998, 1999; Inui and Hanawa 1997; Venzke 1999)? We first identify the source region for the subducting anomalies and then study the local atmospheric forcing fields [Comprehensive Ocean–Atmosphere Data Set (COADS)] to identify the dominant processes that initiate the subducting anomalies.

The next section introduces the datasets and describes the methods used to determine the depth of isotherms. Section 3 discusses the observed mean state and its comparison with LPS83; section 4 describes decadal anomalies of isotherm depths and compares propagation paths with the distribution of potential vorticity. The relative roles of propagation and local wind stress forcing are discussed in section 5 followed by the conclusion and discussion of results in terms of proposed dynamics of decadal climate signals.

2. Data

a. Upper-ocean temperature

All available BT, XBT, and CTD stations were collected and optimally interpolated by White (1995) to a three-dimensional grid of 2° lat by 5° long, 11 standard depth levels between the surface and 400 m, and monthly anomalies from 1955 to 1996. Decorrelation scales of the optimal interpolation are 10° long, 5° lat, and 90 days. In the Pacific data density is sufficient to describe the three-dimensional temperature structure north of 20°S and we use data from 1970 to 1996.

Using the same ocean observations but a different interpolation scheme, DAT96 identified southward propagating cold anomalies in the thermocline during the 1980s. We computed annually averaged anomalies for the same vertical sections as DAT96 and applied a 5-yr filter with linearly varying weights. The White dataset captures the same cold anomaly starting at the surface after 1977 and propagating southward in later years (Fig. 1). As found by DAT96, the cold anomalies appear to increase in amplitude with time. The primary reason for this is that cold (upwelling) thermocline anomalies associated with the 1984–85 and 1987–88 La Niña events (Miller et al. 1997) propagate from the coast of North America westward into the averaging area near 15°–25°N roughly 2 years after their excitation in the tropical Pacific. As described by Miller et al. (1997) and Miller et al. (1998), extended empirical orthogonal function analysis can separate these interannual propagating signals from the decadal-scale subducting signal. Thus, the low-pass filtered anomalies described below and by DAT96 are real and not aliased higher-frequency signals.

The data also show warm anomalies that first appear close to the surface in the early 1970s (Fig. 1) and migrate southward somewhat faster than the cold anomaly. The southward travel of both the cold and warm anomalies follows the mean isotherms 12°–18°C that also straddle the change of SST associated with the 1976–77 climate shift (Fig. 2). This suggests a description of vertical and horizontal propagation of thermal

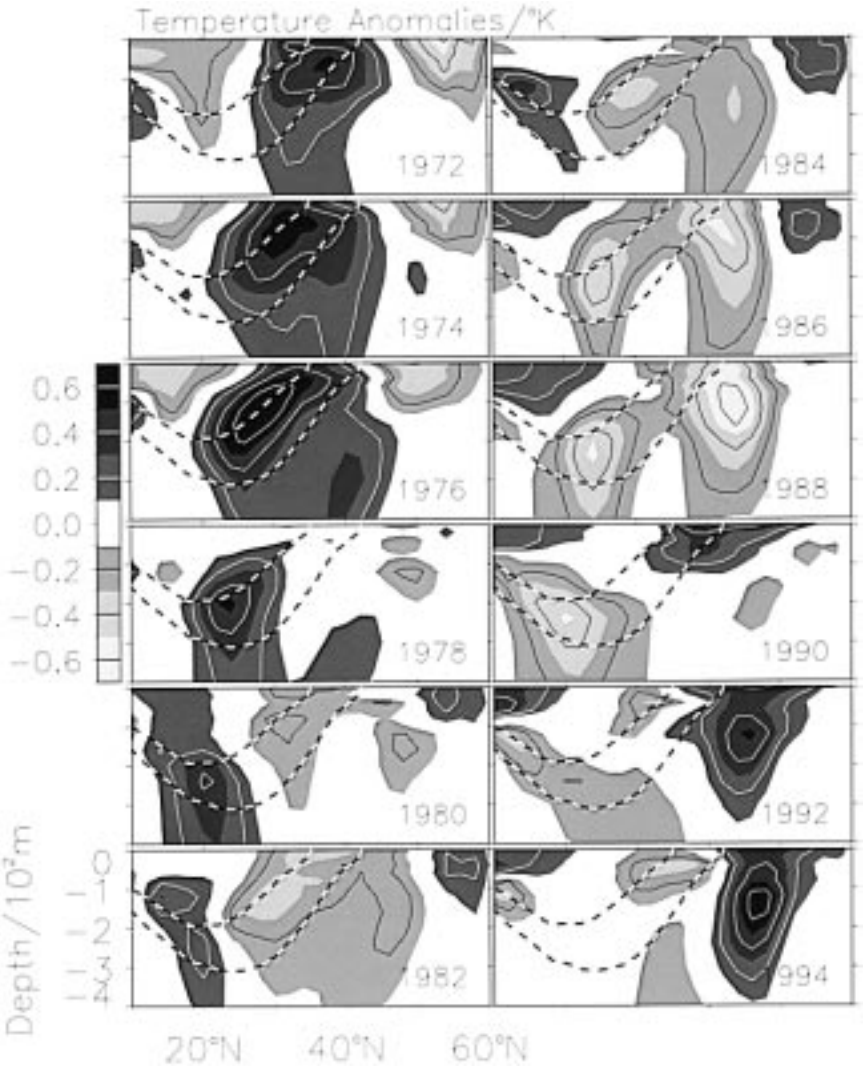

FIG. 1. Filtered decadal temperature anomalies from the White (1995) data analysis in the central North Pacific between 170° and 145°W as a function of latitude and depth and centered on the indicated year. A five-point triangular filter was applied to annual averaged temperature data. The temperature scales in kelvin is given by the gray scale on the left and contour interval is 0.2 K. Superimposed are the 12° and 18°C isotherms of the time-averaged temperature field (dashed lines).

anomalies by mapping undulations of the depth of the 12°–18°C isotherms. Such a description has the added benefit that it lends itself to comparison with the dynamical framework of layers that have been used to explain and explore the thermocline and its variations (Luyten et al. 1983; Pedlosky 1996).

Isotherm depths were calculated using the following procedure. The three-dimensional temperature was reconstructed from the monthly climatology and anomalies. At every horizontal location vertical temperature profiles were sorted to remove temperature inversions that occur quite frequently and were of much smaller magnitude than differences of and shallower than the depth of isotherms of interest. The profiles were then made strictly monotonic with depth by the introduction of an insignificantly small (10^{-4} K m^{-1}) stratification to homogenous levels. Isotherm depths were then obtained by linear interpolation of these vertical temperature profiles. Overall, this procedure is equivalent to determining the mean depth of a particular isotherm in a multivalued profile. Layer thickness is then determined as the difference in depth of the 12°C and 18°C isotherms.

A monthly mean climatology of the isotherm depths was then computed and anomalies were formed with respect to it. To extract low-frequency signals, annual averaged anomalies were smoothed with a five-point filter with linearly decreasing weights (a normalized 1–2–3–2–1 filter) and a half power point at 6.7 yr.

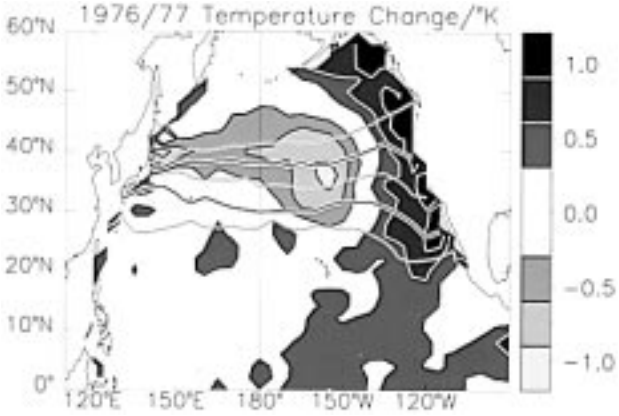

FIG. 2. Surface temperature change associated with the 1976–77 climate change in the North Pacific. Shown as shaded contours is the difference between 1970 to 1974 and 1978 to 1982 based on a reconstruction using the leading EOF of surface temperature anomalies. Shading is explained by the bar on the right and contour intervals is 0.3 K. Superimposed as black lines with white borders are mean wintertime (Jan, Feb, Mar) surface isotherms of 9°, 12°, 15°, 18°, and 21°C. For later reference the 12° and 18°C isotherm are emphasized by a heavy contour.

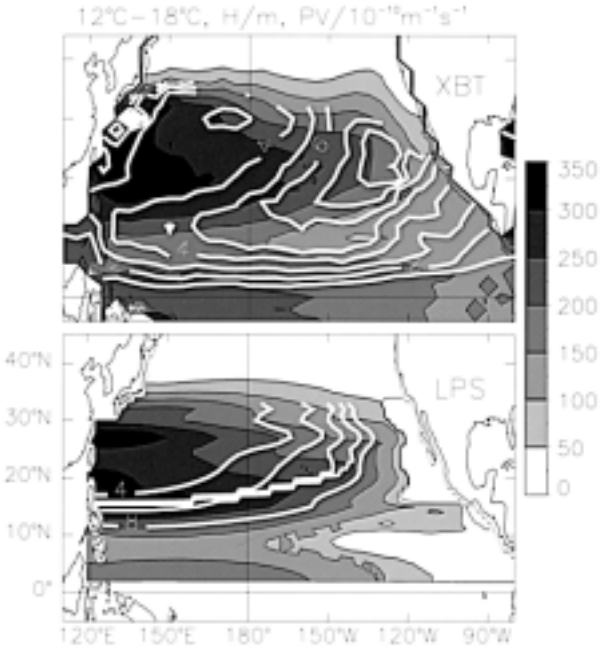

FIG. 3. (Top panel) Average depth of the layer defined by the 12° and 18°C isotherm derived from the White (1995) analysis of temperature in the upper ocean. Depth is given in meters and depicted by gray shading explained by the bar on the right. Depth varies from less than 50 m in the white areas to more than 300 m in darkest areas with a contour interval of 50 m. Superimposed white lines are isolines of potential vorticity of this layer in 10^{-10} m^{-1} s^{-1}. (Bottom panel) The mean depth of layer 2 of a 3-layer model (LPS) of the ventilated thermocline shown in the same gray scale as the top panel. Superimposed are the model's potential vorticity in layer 2. The model (Luyten et al. 1983; Talley 1985) was forced by time averaged Ekman pumping derived from the Da Silva et al. (1994) wind stress. Note that the model captures depth and potential vorticity very well in the ventilated region, but fails to capture the structure of shadow region in the east.

b. SST and atmospheric forcing

In addition to subsurface temperatures, anomalies of surface temperature compiled by the U.K. Hadley Centre were used. This dataset covers the time period from 1930 to the present (Rayner et al. 1996). Also the wind stress product of Da Silva et al. (1994) based on COADS data and covering 1945–92 and surface heat turbulent fluxes computed by Cayan (1992a) from COADS are employed. The latter fluxes were used by Miller et al. (1994a,b) to model the oceanic response to the 1976–77 climate shift and are discussed in detail by them.

3. Mean state depths and potential vorticity

a. Layer depth

Mean depths of the 12°C and 18°C isotherms display a bowl shape in the subtropical gyre and in the transition to the equatorial current system near the edge of the North Equatorial Countercurrent (Fig. 3). The 12°C isotherms outcrop along 38°N with a slight northward slope toward the eastern half of the basin (Fig. 2). The 18°C isotherm outcrops between 35° and 30°N with a southward slope toward the east. South of these outcrop lines the depth of isotherms increases sharply in the west, as expected from the strong zonal currents in the Kuroshio and Kuroshio extension region (Fig. 3), and reach the greatest depths of 400 m at 30°N for the 12°C isotherm and 150 to 200 m at about 20°N for the 18°C isotherm. The mean depth of the layer defined by the 12° and 18°C isotherms exceeds 300 m in the western subtropics. In the eastern half of the basin the layer shoals and forms a region of small depth changes that connect waters off North America with the Tropics. Farther south a ridge in the depth of the layer crosses the Pacific and separates the North Equatorial Current on its northern slopes from the North Equatorial Countercurrent on its equatorward slopes. On the ridge, the 12°C isotherms are shallower than 150 m at 140°W and reach close to 200 m in the western part of the basin. The 18°C isotherm has a similar east–west gradient and varies between 150 m in the west and 50 m in the east. On the equator, the depth of the isotherms show the east–west slope with a deep thermocline in the western Pacific and a shallow thermocline in the upwelling regions of the eastern equatorial Pacific.

b. Potential vorticity

Potential vorticity (PV) in the limit of small Rossby number, in a layered fluid of small aspect ratio, is obtained from

$$\mathrm{PV} = \frac{\Delta\rho}{\rho_0}\frac{f}{\Delta H}, \qquad (1)$$

where f is the Coriolis frequency, ΔH is the layer thickness estimated as the difference of depth of the 12°C and 18°C isotherms, ρ_o is the mean density, and $\Delta\rho$ is the density difference between these two isotherms (e.g., Talley 1988; Pedlosky 1996). Salinity has not been included in the estimation of potential vorticity. This is valid if either temperature dominates density over salinity or if the temperature–salinity relationship is a constant so that horizontal gradients of temperature and density are parallel. Experiments with data of Levitus (1982) show that, in the North Pacific away from the eastern boundary, potential vorticity based on isotherms and isopycnals correspond closely.

Lines of constant potential vorticity (Fig. 3) emanate from the outcrop region of the layer in the north Pacific and form a closed region in the west, reminiscent of the Rhines and Young (1982) homogeneous pool of potential vorticity. From the outcrop regions east of the date line, lines of constant PV extend southward, swing toward the west, and identify the ventilated region (LPS83). Potential vorticity lines that emanate from the eastern boundary swing toward the west and delineate the shadow zone to the east of a potential vorticity maximum. South of 10°N the potential vorticity barrier described by McCreary and Lu (1994) associated with the North Equatorial Countercurrent is seen, and toward the equator potential vorticity decreases due to the decrease of f. However, for the very low latitudes, planetary vorticity is no longer dominant over relative vorticity of the mean flow (the Rossby number is no longer small compared to one), and Eq. (1) is no longer valid. These results are in broad agreement with results with Talley (1988) even though a detailed comparison is difficult because of the coarse resolution of isotherms.

c. Application of the ventilated thermocline

To establish our dynamical framework and for later application to observations of the anomalous layer depths, we compare observed mean layer depth and potential vorticity with the predictions of the ventilated thermocline (LPS83; Talley 1985). This model predicts the time-independent thickness of three active layers overlying a deep motionless ocean based on conservation of potential vorticity and the Sverdrup balance. It has previously been successfully applied to the time mean circulation of the North Pacific (Talley 1985). Parameters required are average densities of the layers, reduced gravities between layers, latitudes of outcrop lines, and the depth of the lowest active layer at the eastern boundary. Densities are estimated from the Levitus (1982) climatology for waters above 1500 m. The density of layer 1 is defined as the average density of waters warmer than 18°C, layer 2 by temperatures between 12° and 18°C, and layer 3 by temperatures between 12° and 6°C. Reduced gravities are determined from the density differences between the layers. The depth of the lowest active layer at the eastern boundary was determined from Levitus (1982) as the depth of the 6°C isotherm off California. In the solution of the ventilated thermocline of LPS83 and Talley (1985) the outcrop lines are zonal. Their latitudes are determined here from the winter surface conditions of the North Pacific of the climatological temperature data based on White (1995). The resulting parameters are listed in Table 1.

TABLE 1. Parameters for the three-layer thermocline model (Luyten et al. 1983; Talley 1985). The outcrop latitudes were chosen from the (Jan–Mar) outcrops of the respective isotherms in the North Pacific from the White (1995) temperature dataset. Reduced gravities were obtained from Levitus by averaging densities of the North Pacific above 1500-m depth that correspond to temperatures within the layer bins. The undisturbed depth of layer three of 600 m was determined from the Levitus data as the depth of the 6°C isotherm in the eastern subtropical Pacific.

Layer	Outcrop latitude	Reduced gravity (m s^{-2})	Minimum temperature (°C)
1	33°N	$15\cdot10^{-3}$	18
2	41°N	$9\cdot10^{-3}$	12
3	—	$7\cdot10^{-3}$	6

The solution of the mean ventilated thermocline simulates the mean depth of the layer defined by the 12° and 18°C isotherms very well in the ventilation region and western North Pacific, including the position, southwestward swing, and magnitude of the potential vorticity isopleths (Fig. 3). Observed average layer depth and potential vorticity isopleths to the south of the ventilation region are not well captured by the model. Inclusion of the eastern boundary ventilation of layer 2 would generate a ridge of high potential vorticity at the eastern edge of the ventilation region and deepen the equatorial layers (Pedlosky 1983) in agreement with observations. However, this arduous extension of the analytic theory suggested by Pedlosky (1983) was not attempted since the region of ventilation from the outcrops in the north Pacific, the main focus of this work, is well reproduced.

4. Decadal anomalies

Anomalies in the depth of the layer defined by the 12° to 18°C isotherms are estimated as an average of the depth anomalies of the 12°, 15°, and 18°C isotherms. The signal described below is consistently found in each of the isotherms and the average is chosen to increase the clarity of the presentation.

Root-mean-square values of low-frequency depth anomalies (derived by application of the five-point filter to annually averaged anomalies) from 1970 to 1996 (Fig. 4, top panel) show that variability occurs in three regions delineated by the mean potential vorticity structure. Rms values are large in the Kuroshio Extension where potential vorticity has small gradients, in the ventilation region of the thermocline defined by values of mean potential vorticity between 3.5 and 6.5 ($\times10^{-10}$

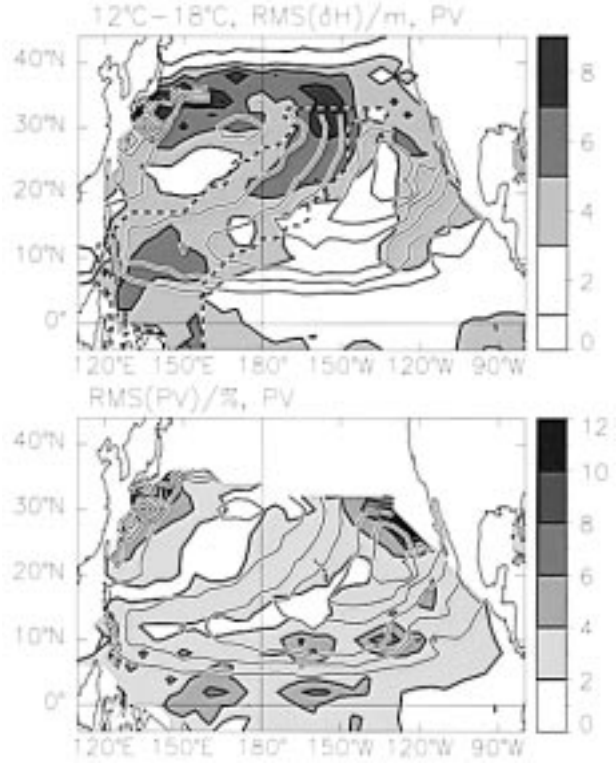

FIG. 4. Rms values of decadal depth anomalies of the 12°–18°C layer (in m) with a contour interval of 2 m (upper panel) and of anomalies of layer thickness normalized by the mean thickness in percent with a contour interval of 2% (lower panel). The latter quantity is a measure for the anomalous perturbation vorticity. Values of decadal depth anomalies larger than 3 m (top panel) and values of the relative thickness change larger than 2% (bottom pane) are shaded. Black lines with white borders show the mean potential vorticity of the layer, and the white and black dashed line in the upper panel surrounds a region over which depth anomalies are zonally averaged in Fig. 6. It is designed to capture the large variance of the depth anomalies. Poleward of 15°N it corresponds to the ventilation region defined by values of the mean potential vorticity between 3.5 and 6.5 ($\times 10^{-10}$ m^{-1} s^{-1}).

m^{-1} s^{-1}) extending from the central North Pacific to the tropical western Pacific, and in the shadow zones of the eastern North Pacific where potential vorticity lines originate at the coast of North America. The elevated rms values in the shadow zone are predicted by Liu (1996) as a Rossby wave response to changes of the Ekman pumping, while Liu and Pedlosky (1994) suggest that variability in the ventilation region results primarily from changes of the surface temperatures in the subduction region. The variability in the Kuroshio Extension is consistent with the spinup of the gyre in response to decadal changes of the wind stress curl (Miller et al. 1998; Deser et al. 1999).

The depth anomalies in the ventilation region propagate southwestward from the outcrops in the central north Pacific to the western tropical Pacific (Fig. 5). In 1972 a positive depth anomaly, corresponding to a warm signal, existed north of Hawaii in the outcrop region of the 3.5 to 6.5 ($\times 10^{-10}$ m^{-1} s^{-1}) potential vorticity contours. This anomaly strengthened in 1974 to achieve values in excess of 15 m in 1976, moved from 1974 to 1980 in a southwestward direction along lines of constant potential vorticity, and disappeared at 20°N in 1982. In the western Pacific south of 20°N a warm anomaly with depth anomalies of up to 9 m existed from 1974 to 1978 that cannot be traced to the subduction region in the central North Pacific.

Starting in 1980, a negative depth anomaly, corresponding to cold conditions, appeared in the subduction region in the central North Pacific. This anomaly strengthened in 1982 and possibly 1986 to values of 9 m and moved along lines of constant potential vorticity. From 1984 to 1990 the signal propagated toward the western Pacific in a southwestward direction along lines of constant potential vorticity and reached the western Pacific south of 20°N in 1990. From 1990 to 1994 it appears that the signal spreads to the equatorial western Pacific and increases in magnitude to as large as 15 m while the zonal tilt of the equatorial thermocline is reduced by a deepening in the eastern equatorial Pacific. However, we will show in the following that the large anomalies in the western Pacific are a response to tropical wind forcing and not due to propagation of the midlatitude signal to the equator.

The southward propagation and travel time can be seen most clearly by averaging the depth anomalies zonally in the ventilation region (shown by the dashed line in Fig. 4) that, poleward of 15°N, correspond to the area between the mean potential vorticity lines of 3.5 and 6.5 ($\times 10^{-10}$ m^{-1} s^{-1}). The southward propagation has a meridional speed of approximately 7×10^{-3} m s^{-1} and a travel time from the subduction region north of Hawaii at 35°N to the western Pacific of approximately 8 yr (Fig. 6). The propagation compares very well with advection by geostrophic currents between the 12° and 18°C isotherms and by the circulation predicted by the model of the ventilated thermocline. Meridional geostrophic velocities from the geostrophic current relative to 1500 m from Levitus (1982) data and from the solution of the ventilated thermocline (Fig. 3) were zonally averaged over the ventilation region (Fig. 4) and integrated in time to yield the paths in Fig. 6.

In contrast to anomalies of layer depth, anomalies of potential vorticity do not show any coherent signals. Rms values of the ratio of layer thickness anomaly and the time-averaged layer thickness, a measure for the perturbation potential vorticity [see Eq. (1)], are less than 5% (Fig. 4) and do not show any coherent propagation (not shown). Despite the small values, the rms of perturbation PV are elevated along the western boundary, ventilation region, and in the eastern shadow zone (Fig. 4). The small values of the perturbation PV suggest the possibility of linearization of the dynamics around the mean state and indicates that the perturbation forcing is small compared to the mean forcing. Also, the usual ventilated thermocline analysis approach of

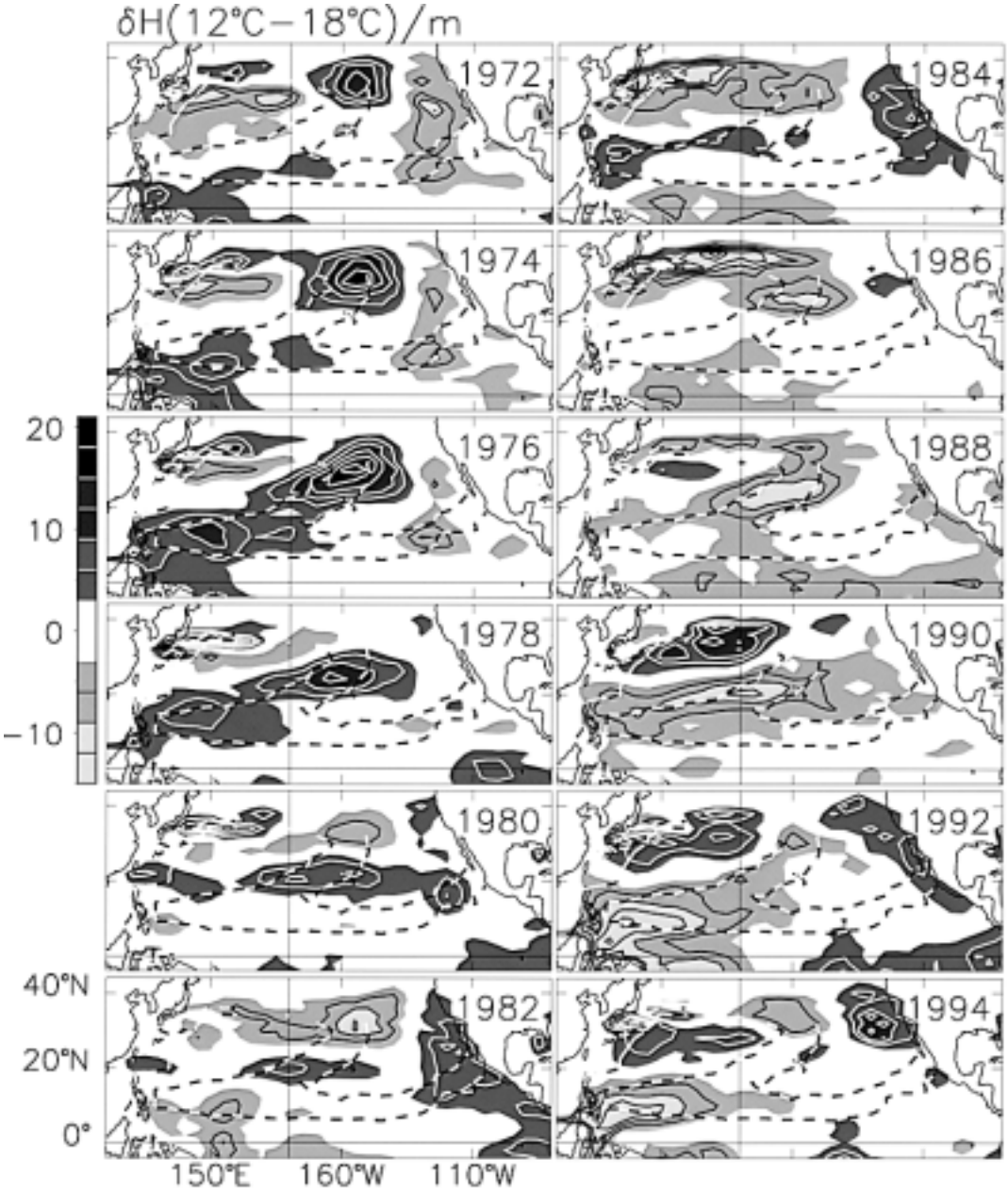

FIG. 5. Decadal anomalies in the North Pacific of the depth of the 12°–18°C layer for years 1972 to 1994. Annual averaged anomalies were smoothed with a filter with linearly varying weights over a 5-yr interval. Dark shaded areas mark positive anomalies larger than 3 m, corresponding to anomalous large depth of the layer and warm conditions, light gray shading denotes negative depth anomalies in excess of −3 m and correspond to cold conditions (see gray scale on the left). Contour interval is 3 m, and the zero contours are not shown for clarity. Overlaid as dashed lines are the 4 and 6 × 10^{-10} m^{-1} s^{-1} contours of the mean potential vorticity (e.g., Fig. 3).

estimating PV anomalies on constant density surfaces is difficult due to the small amplitude of PV anomalies.

In summary, the data show a clear propagation of thermal signals along isopleths of mean potential vorticity from the subduction region in the central North Pacific north of 33°N to the tropical western Pacific to 18°N, while the perturbations of potential vorticity are small. The meridional speed of the signals (~7 mm s^{-1}) closely matches advection by geostrophic currents and the solution of the ventilated thermocline driven by the time-averaged winds. These findings strongly suggest that poleward of 18°N the perturbations are carried by the mean circulation, which is governed by dynamics of the ventilated thermocline. Equatorward of 18°N the correspondence between the propagation of thermal anomalies and the predictions by the ventilated ther-

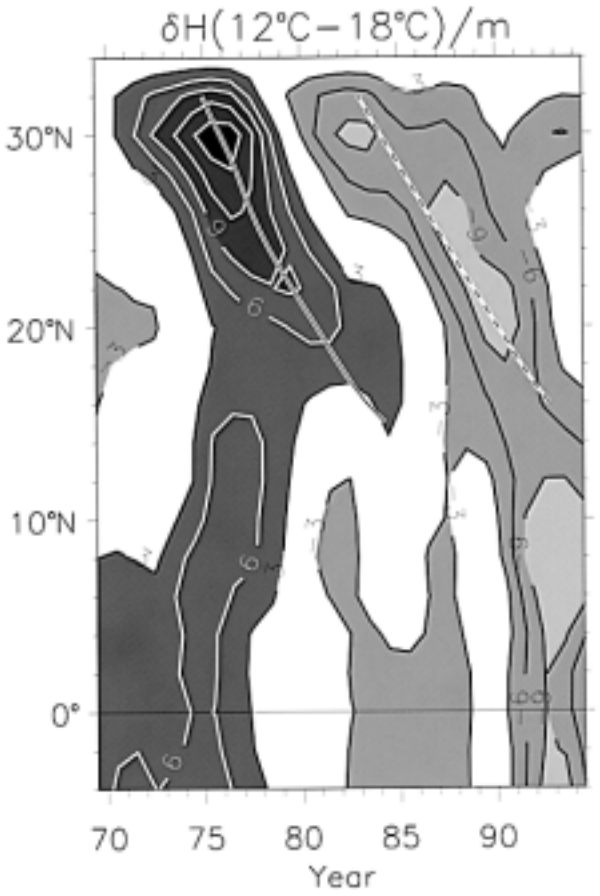

FIG. 6. Zonal average of decadal anomalies of the depth of the 12° to 18°C layer in meters as a function of year and latitude. Average was performed in the region denoted by a black and white dashed line in Fig. 4. The black line on white background denotes the path of a particle advected by the zonally averaged meridional speed in the same region but predicted from the model of the ventilated thermocline forced by average of observed mean winds from 1969 to 1993. The dashed line on white background shows the path of such a particle advected with the geostrophic flow relative to 1500 m based on the Levitus (1982) data.

mocline fails and suggests that local forcing is important.

5. Surface forcing

The propagation of thermal anomalies in the thermocline begs the question of how these are forced in the outcrop region and whether their propagation and growth in the tropical Pacific could be influenced by tropical Ekman pumping. To investigate these issues, surface forcing in the source region in the central North Pacific and the Ekman pumping affecting the areas visited by the propagating anomalies are investigated using COADS-based surface forcing from Cayan (1992a) and from Da Silva et al. (1994). In the following, we define the subduction source region as 28°–38°N, 155°–125°W.

a. Surface fluxes in outcrop region

Consider the equation for temperature T in oceanic surface mixed layer of depth H,

$$\frac{\partial}{\partial t}T = -\mathbf{u}\cdot\nabla T + \frac{Q}{H\rho_0 c_p} - \frac{w_e}{H}\Delta T, \qquad (2)$$

where the left-hand side describes the time (t) rate of change of temperature. The right-hand side represents advection by mixed layer velocity $\mathbf{u}$, turbulent fluxes into the mixed layer due to the surface heat flux Q, normalized by the ocean density ρ_0 and ocean's specific heat c_p, and due to entrainment velocity w_e importing water into the mixed layer across its base with temperature jump ΔT. In midlatitudes, variations of the surface heat flux are generally the largest contributor to SST anomalies in winter (e.g., Frankignoul 1985; Cayan 1992b), the time when properties of subducted waters are set (Cushman-Roisin 1987). Other important processes affecting SST anomalies are variations in mixing and advection by ocean currents. These two processes are predominantly controlled on seasonal timescales by anomalous wind speed and Ekman currents, respectively (e.g., Miller et al. 1994b). We evaluate the magnitude of these three forcing effects on (2) in the following way. Assuming the mixed layer to be of constant depth (H = 100 m) in the winter months of January–March, the heat flux term was approximated as $Q'(\rho_0 c_p H)^{-1}$, the mixing term as $w_e'\Delta T H^{-1}$, and the Ekman advection term as $\mathbf{u}_e'\cdot\nabla T^M$. Here, Q' is the January to March (JFM) seasonal mean total surface heat flux anomaly (Cayan 1990), ρ_0 = 1025 kg m^{-3}, c_p = 4180 J kg^{-1} K^{-1}, $\mathbf{u}_e'$ is the Ekman velocity anomaly averaged over the mixed layer and T^M is the mean SST computed from COADS. Ekman pumping is evaluated as the divergence of the Ekman currents (wind stress curl plus the beta term: Gill 1982) from a blend of the COADS wind stress with FSU wind stress (Miller et al. 1994b). Anomalous entrainment heat flux was determined from the turbulent kinetic energy balance between wind stirring, proportional to wind friction velocity cubed (u_e^3, estimated according to Miller et al. 1994b) and the increase of potential energy due to the entrainment heat flux.

The time series of these anomalous winter SST heat budget terms reveal intervals of strong or persistent anomalous forcing in the subduction source region (Fig. 7). All three terms in the heat budget act to warm the source region in the years 1973–76 when the warm anomaly of layer depth was formed (Fig. 7). After 1976, a series of anomalous severe winters, interrupted by years of near normal or warm conditions, coincide with the appearance of a cold depth anomaly in the source region. The total cooling during this period is dominated by the anomalous severe winter associated with the 1982–83 El Niño such that the total forcing during the warm periods and the winter of 1982/83, normalized to account for the different duration, are of equal magnitude but opposite sign. The anomalous wintertime cool-

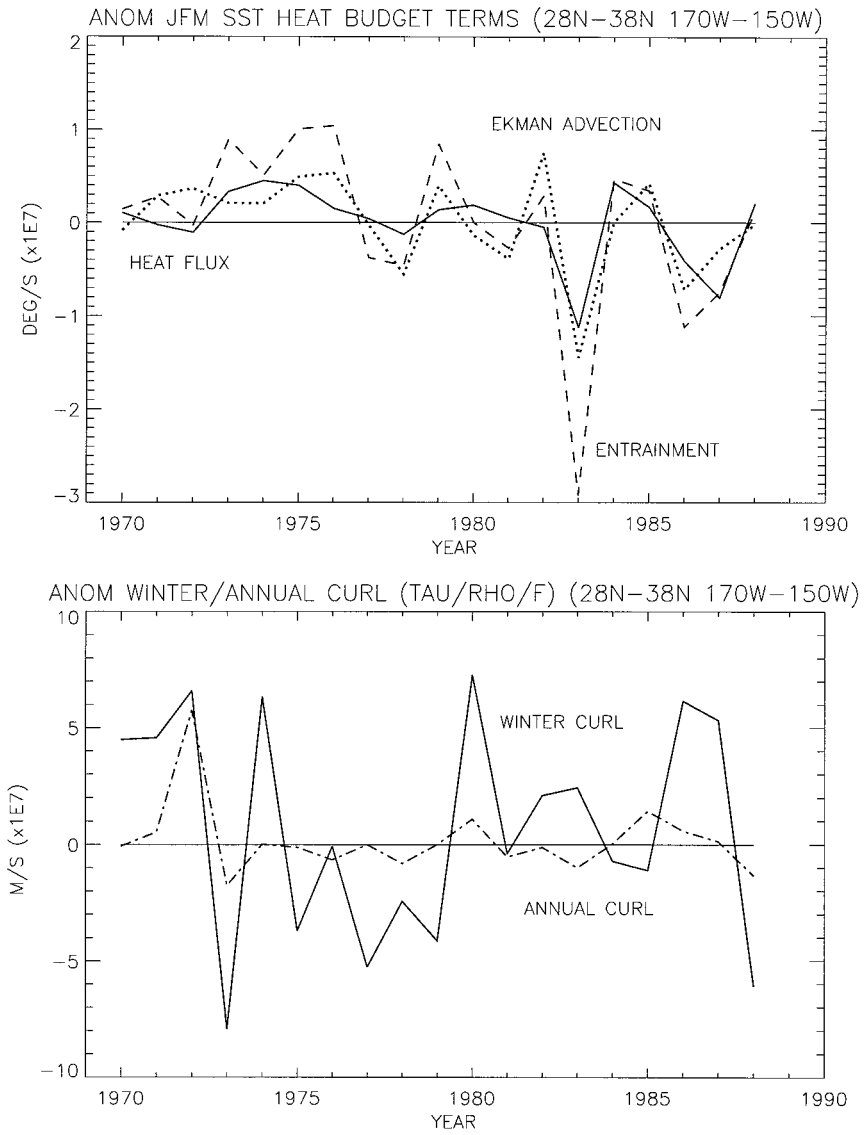

FIG. 7. (Top panel) Time series of anomalous heat budget terms in 10^{-7} K s^{-1}. Solid line denotes anomalies of surface heat flux, dashed line denotes entrainment, and dotted lines denotes Ekman advection. (Bottom panel) Time series of divergence of Ekman pumping in 10^{-7} m s^{-1} in the ventilation region of the 12° to 18°C layer. Solid line is winter (Jan–Mar) and dash-dotted is annual average.

ings are dominated by the entrainment heat flux, that is, by changes of the wind friction velocity, consistent with changes of the zonal wind speed reported by DAT96 and the changes of Ekman advection. In addition, the cooling episodes in the winters of 1980/81, 1982/83, and 1986/87 are associated with the occurrence of El Niño and suggest that the anomalous atmospheric conditions are communicated to the North Pacific via atmospheric teleconnections (Alexander 1992; Lau 1997). The anomalous Ekman pumping on the other hand has large year-to-year changes, but no signals (for either annual or winter anomalies) that are coincident with the occurrence of anomalies of the 12°–18°C layer depth (Fig. 7).

Comparisons of the spatial patterns of these heating terms averaged over 1974–76 and for the winter of 1982/83 show that the subduction source region is close to extrema of heat flux, of flux of turbulent kinetic energy, and of zonal wind stress. In contrast, the source region straddles the nodal line of anomalous Ekman pumping (Fig. 8). Moreover, south of the source region the Ekman pumping acts in the opposite sense of the observed anomalies, for example, downwelling during the cold subducting phase. Thus it appears that oceanic

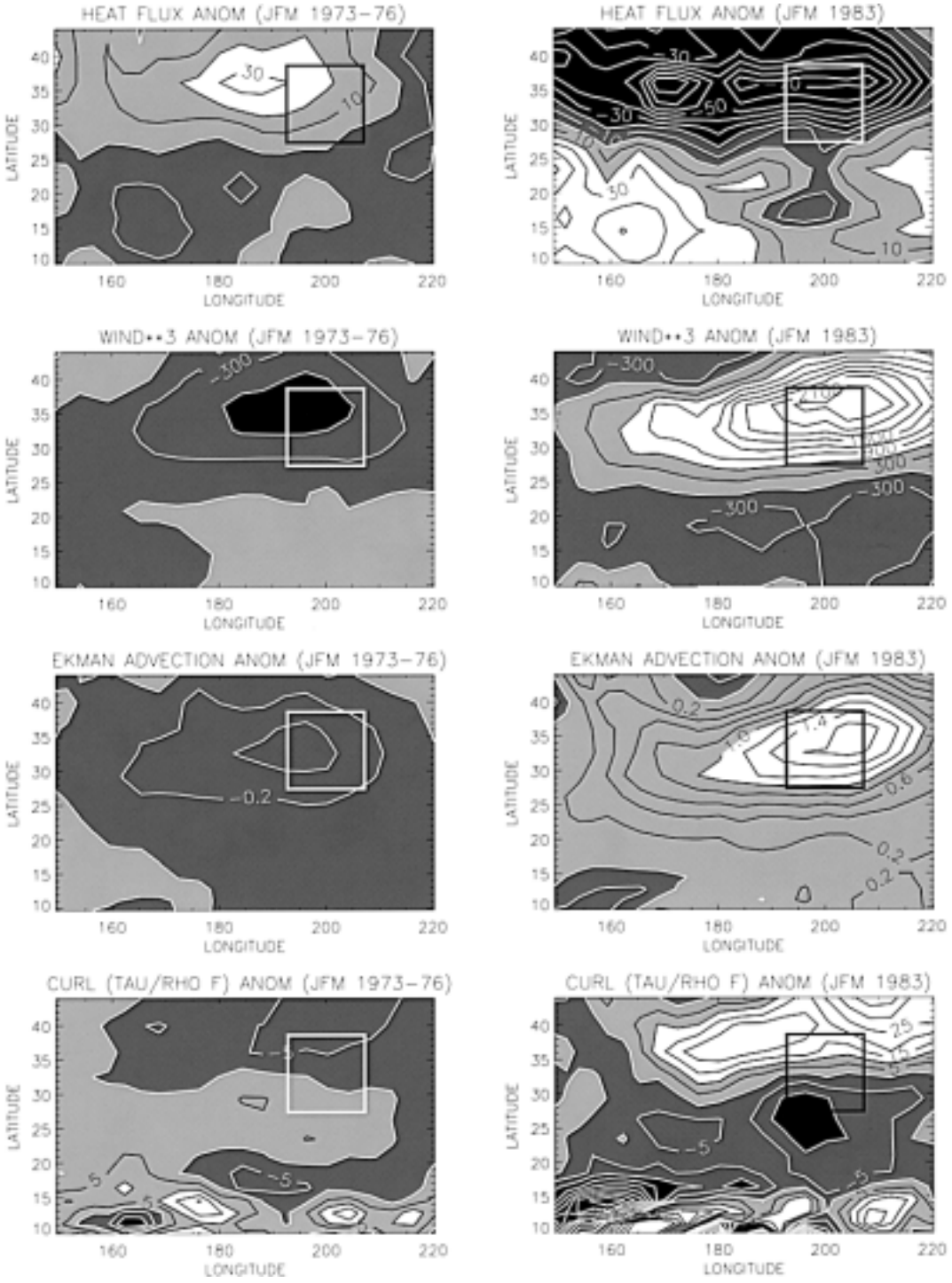

FIG. 8. Anomalies of surface forcing for winters of 1973–76 (left column) and winter 1982/83 (right column) in the North Pacific derived from the COADS and FSU databases. Shown are anomalies of fluxes of heat in W m^{-2} (top row), flux of turbulent kinetic energy measured by wind speed cubed in $m^3\ s^{-3}$ (second row), heat advection by Ekman currents in K s^{-1} (third row), and Ekman pumping in 10^{-7} m s^{-1} (bottom row). The solid box shows the region where the 12° to 18°C layer ventilates.

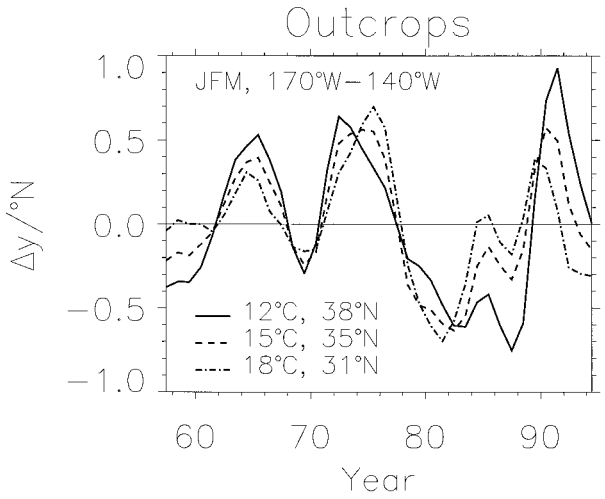

FIG. 9. Time series of outcrop latitude of 12°, 15°, and 18°C winter isotherms (Jan, Feb, Mar) averaged from 170° to 140°W. Data is based on surface XBT data. Legends denote average latitudes of isotherms at the surface during winter.

thermal anomalies that originate in the source region are generated by diabatic surface forcing, that is, surface heat flux and entrainment and Ekman advection.

It is noteworthy that nature provides two distinct scenarios for the generation of the subducting anomalies: the warm anomaly is a response to persistent anomalous heating over several successive winters, while the cool anomaly results from a series of anomalously severe winters interrupted by near normal or warm conditions. It is interesting to speculate that the action of Stommel's demon (Pedlosky 1996; Williams et al. 1995; Stommel 1979) requires that forcing of a warm anomaly has to last several years to allow anomalies to subduct and escape the influence of a subsequent harsher winter. In contrast, an anomalously cold winter with deep mixed layers can generate subducted anomalies that are insulated from subsequent milder winters and are therefore likely to persist and propagate into the main thermocline. Lastly, the unique winter of 1976/77 associated with a climate shift of the midlatitude North Pacific does not stand out as a key forcing period of the observed subducting anomalies. It serves, however, as a transition point for modulating the effects of interannual variations in forcing, allowing a preponderance of warming events in antecedent years versus cooling events in subsequent years.

b. Variation of outcrop latitude

Diabatic forcing and Ekman advection in the source region affects the SST and leads to displacements of the outcrop latitudes of the 12° to 18°C layer. Since the mean meridional SST gradient is large in the source region (Fig. 2), surface temperature anomalies of 1°C are equivalent to variations of the outcrop latitudes of less than a degree of latitude (Fig. 9). From 1970 to 1978 the winter position of these isotherms was located half a degree farther northward than average, and then shifted southward during the 1980s. In the early 1990s the isotherms moved again northward by over one degree of latitude from its position in the 1980s.

c. Sverdrup transport

The observations presented suggest a propagation of decadal signals from the mid-latitude North Pacific to the subtropical western Pacific. However, the appearance of a warm anomaly at 10°N in the western Pacific from 1974 to 1978 was apparently unconnected to propagation from the midlatitudes. Likewise, the strong growth of the cold anomaly in the western Pacific after 1990 (Fig. 5) does not favor the advection mechanism but instead suggests that vertical displacements of the layer caused by local or remote wind forcing may be important. To test this hypothesis the interface displacement associated with Sverdrup transport (Gill 1982) was estimated from Da Silva et al. (1994) winds, annually averaged from 1969 to 1993 and subjected to a 5-yr filter with linearly varying weights.

Deviations of the thermocline depth expected from the Sverdrup transport alone do not show any relationship with the observed undulations of the 12° to 18°C layer depth north of 18°N (cf. Fig. 6 with Fig. 10) and suggest that observed thermal signals are indeed propagating and not locally forced. South of 20°N the steady oceanic response to wind stress forcing is similar to and precedes oceanic observations by approximately one year (Fig. 10). This lag is expected from the adjustment time of the low-latitude ocean via Rossby waves and suggests that the observed thermal signals are a response to zonally integrated Ekman pumping.

d. Ocean response to Ekman pumping and variation of outcrop latitude

The results so far indicate that the anomalies in the thermocline are forced by the wind stress to the south of 18°N, while the anomalies in the latitude of the outcrop line due to diabatic forcing and Ekman advection might generate subsurface temperature anomalies in the ventilation region between the source region and 18°N. To test this hypothesis, the ventilated thermocline model of LPS83 and Talley (1985) was applied under the assumption of instantaneous adjustment to the time varying forcing. The model was forced by filtered Da Silva et al. (1994) winds and outcrop line variations from 1970 to 1992 and the subsurface depth anomalies from the time-average state were calculated. In all experiments the potential vorticity of the western pool in layer 3 (Talley 1985) was held constant to focus on the dynamics in the ventilation region.

Zonal averages over the ventilated region (Fig. 4) show that the large anomalies south of 18°N can be largely explained by anomalous Ekman pumping at

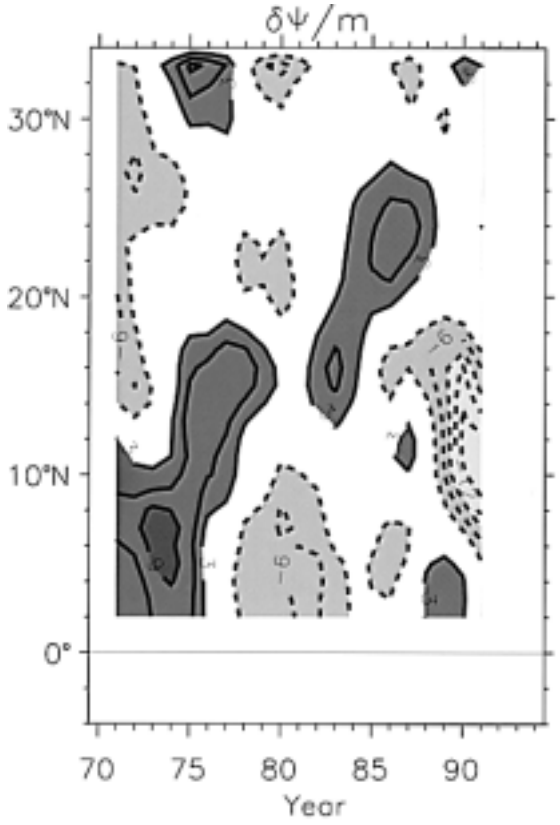

FIG. 10. Anomalies of thermocline displacement in meters due to Sverdrup transport. Sverdrup transports were estimated from the Da Silva et al (1994) wind stress data for each year from 1969 to 1993 and filtered with a 5-yr running mean with linearly varying weights. Transports were converted to displacements by assuming a reduced gravity of 1.6×10^{-2} m^2 s^{-1}. Anomalies from the time average were zonally averaged in the ventilation region (Fig. 4) and results are displayed as a function of time and latitude.

these latitudes (Fig. 11) as seen previously in the calculation of the Sverdrup transport (Fig. 10). However, wind-stress-induced signals north of the 18°N are smaller and cannot explain the observations (Fig. 6). On the other hand, variations of the outcrop latitude (Fig. 9) affect areas to the north of 18°N. Changes there are in phase with the observed depth anomalies, suggesting the importance of forcing by displacements of the outcrop lines. The preponderance of forcing of decadal anomalies in the ventilated region of the ocean by diabatic forcing and Ekman advection as compared to Ekman pumping is consistent with theoretical predictions of Liu and Pedlosky (1994) and Liu (1996).

Note that propagation of subducted anomalies cannot be seen in Fig. 11 because it represents a final steady state to outcrop line changes and not the time-dependent adjustment process observed in nature. It is nevertheless remarkable and attests to the relevance and skill of the model of the ventilated thermocline that the southward penetration limit of the instantaneously adjusted isotherms of the simple model closely matches the observations.

6. Discussion and conclusions

We have presented an analysis of observed long-term anomalies in the thermocline of the North Pacific. In contrast to earlier studies, the description of thermal anomalies by undulations of the depth of isotherms allowed a succinct tracing of the propagation of the thermal anomalies and lends itself to a comparison with predictions of the ventilated thermocline model. Specifically, we focused on the layer bounded by the 12° and 18°C isotherms since it outcrops in the central North Pacific in a key region noted for large decadal changes of sea surface temperature. Results of the study are:

- Decadal variance of the anomalies of the layer depth is large in three regions that are distinguished by their potential vorticity (PV) contours: The Kuroshio Extension region in the western North Pacific north of a pool of nearly homogenous PV, the ventilation region from the central North Pacific east of the date line extending to the tropical western Pacific, and the shadow zone where isopleths of PV originate at the eastern boundary.
- In the early 1970s a warm decadal anomaly originated in the central North Pacific and propagated toward the western subtropical Pacific. In the early 1980s a cold anomaly was generated in the central North Pacific and propagated along a similar path to the western subtropical Pacific. Upon arrival in the subtropics, the cold signal strengthened and appeared to spread throughout the equatorial western Pacific.
- The propagation occurred along isopleths of average potential vorticity. Its speed of 7 mm s^{-1} is well described by the mean advection predicted by the ventilated thermocline forced by observed wind stress. The travel time from the central North Pacific to the subtropical western Pacific is approximately eight years.
- Anomalies of potential vorticity are at most a few percent of the mean potential vorticity and suggest that dynamics are governed by a linear perturbation of the background state.
- North of 18°N thermal anomalies are forced by diabatic processes and Ekman advection that shift the outcrop lines of a layer by typically one degree of latitude.
- Equatorward of 18°N thermal anomalies are primarily forced by the wind stress curl and do not originate from the North Pacific.

In summary, decadal anomalies are forced by diabatic processes and Ekman advection in the subduction region of the central North Pacific are swept toward the subtropical western Pacific with the mean circulation and arrive there approximately eight years later. Anomalies equatorward of 18°N are forced by low-latitude wind

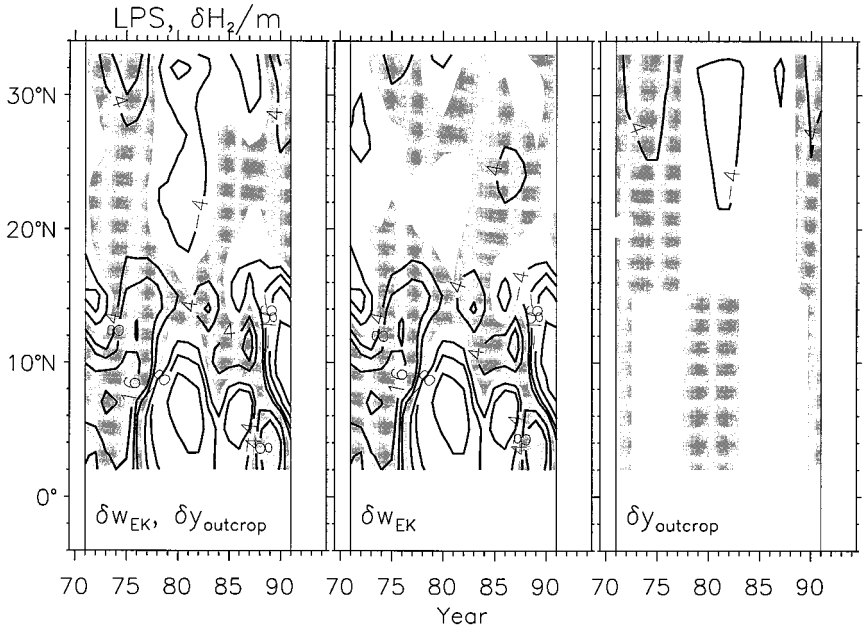

FIG. 11. Depth of layer two of the ventilated thermocline (Luyten et al. 1983; Talley 1985) forced by annually averaged Ekman pumping from 1970 to 1992 and changes of the outcrop latitudes as given in Fig. 9 (left panel). Shown is the deviation from the mean state during the forcing period. Positive anomalies are shaded and the contours are drawn for ±4, 8, 16, and 32 m. Center panel shows the results if only changes of the surface Ekman pumping are considered while the outcrop latitudes remain at their climatological position. The left panel shows changes of depth of layer 2 if the outcrop latitudes are changed only, while the Ekman pumping remains constant. In all of the calculations, the potential vorticity of layer 3 in the western ''homogenous pool'' was held constant.

stress curl. This implies that propagation of thermal anomalies from the midlatitudes cannot explain anomalous warm conditions at the surface and reduced zonal slope of the equatorial thermocline (Fig. 5) observed in the equatorial Pacific in the early 1990s. These results are largely consistent with observational analyses reported by Tourre et al. (1999) and Zhang and Levitus (1997), but we have been able to demonstrate the physics of the subducted anomalies and their confinement to the midlatitudes and subtropics.

These results are inconsistent with the hypothesis that the decadal timescale results from propagation of anomalies from the midlatitudes to the equatorial region (Gu and Philander 1997) and the observational analysis of Zhang et al. (1998). However, the development of Ekman pumping south of 18°N just at the time when the cold anomaly from midlatitudes arrives could indicate a possible, albeit tenuous, linkage. The equatorial response could be due to the midlatitude signal if the upward shift of isotherms in the thermocline associated with the cold anomaly affects sea surface temperature in the western tropical Pacific through perturbations of the surface layer heat budget and if the resulting atmospheric response induces the Ekman pumping that strengthens the signal and communicates it to the equatorial region. Alternatively, the arrival of the subducted signal in the western tropical Pacific could be communicated to the equatorial region via coastal Kelvin waves (Lysne et al. 1997) or the western boundary currents (McCreary and Lu 1994) and initiate positive feedbacks in the atmosphere there. In either case, decadal anomalies of sea surface temperature in the midlatitude source region should be correlated with decadal anomalies in the Tropics at a lag of 8 to 10 years. The correlation of decadal anomalies in the source region and in the central equatorial Pacific eight years later is 0.23, not significant at the 95% confidence level (0.55 for a charitable estimate of ten degrees of freedom). The correlation is significantly smaller than the correlation of SST anomalies in the central equatorial Pacific with the Sverdrup streamfunction in the western Pacific of -0.73 (Fig. 12). This suggests that local forcing in the equatorial region is the main driving force and largely independent of the arrival of thermal signals from the central north Pacific. Thus, the data do not support significant coupling of the midlatitudes and Tropics via anomalous subduction from the central north Pacific along the oceanic thermocline.

The theoretical study of McCreary and Lu (1994) and the simulation of Rothstein et al. (1998) suggest that the location of origin of subducted particles in the North Pacific determines if these are either recirculated in the subtropical gyre or penetrate to the equatorial region via low-latitude western boundary currents or via a mid-

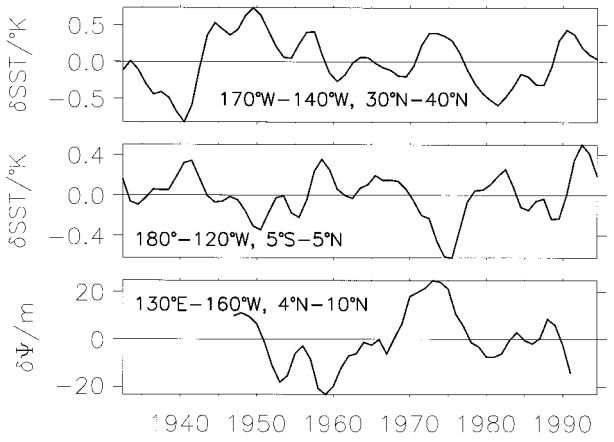

FIG. 12. Time series of winter surface temperature in the ventilation region of the 12°–18°C layer (top panel), sea surface temperature anomalies in the central equatorial Pacific (center panel), and anomalies of the transport stream function in the western tropical Pacific (bottom panel). The decadal signals are extracted by application of a 5-yr filter with linearly varying weights after removal of the mean trend. Correlations are highest between SST in the equatorial Pacific and stream function (−0.73). In contrast, the correlation of 0.23 between SST anomalies in the central North Pacific and in the equatorial Pacific at a lag of eight years (north Pacific leading) is not significant at the 95% confidence level. This weak lag correlation between SST in the north and the equatorial Pacific is inconsistent with the notion that strong coupling between the midlatitude North Pacific and equatorial regions by way of the advection in the oceanic thermocline.

ocean pathway. Thus thermal anomalies that originate to the east or south of the central north Pacific could communicate the decadal signal between the midlatitudes and the equator. However, decadal anomalies of the 12°–18°C layer that originate east of 135°W do not show any coherent southward propagation (Fig. 5). Similarly, depth anomalies of isotherms that are warmer and outcrop on the southern flanks of the decadal midlatitude change (Fig. 2) do not display coherent propagation that is independent of those discussed (not shown). The data also provide no evidence that the thermal anomalies return to the midlatitudes via the western boundary current. This, however, might be due to the optimal interpolation used in preparation of the dateset (White 1995) that discriminates against small spatial scales such as might be expected from changes of temperature and transport of the western boundary current. Finally, the possible coupling of the equatorial region with the data-poor midlatitudes of the Southern Hemisphere remains to be investigated.

The subducted thermal anomalies originating in the central North Pacific appear to be distinct from the thermal signal associated with the acceleration of the North Pacific gyre circulation. Miller et al. (1998) and Deser et al. (1999) document that the increase in wind stress over the North Pacific from the 1970s to 1980s led to a spinup of the subpolar and subtropical gyres in accordance with Sverdrup theory. Associated with this spinup are western-intensified thermal anomalies extending down to at least 400 m in the Kuroshio Extension that can be seen in Fig. 1 between 40° and 50°N. The importance of this gyre spinup and the thermal anomalies within the thermocline for a mechanism of decadal oscillations ''à la Latif and Barnett (1994, 1996)'' remains to be determined.

The propagation and forcing of the thermal anomalies in the thermocline bear striking resemblance to the second-mode motions in the thermocline discussed by Liu (1999a). This is yet another piece of evidence that dynamics of the ventilated thermocline are at the heart of the dynamics of decadal anomalies in the midlatitude North Pacific thermocline. However, due to the lack of salinity observations we cannot say whether the subducted temperature anomalies are salinity compensated (with no anomalous velocity field) or are high-mode baroclinic waves (which have anomalous velocity) whose propagation path and speed are close, but not identical, to advection by the mean circulation. Efforts by T. Suga (1997, personal communication) to obtain adequate historical salinity observations may resolve this issue. The statistical significance of the analysis presented here is obviously limited by the small number of observed realizations. Analysis of targeted experiments with numerical models (Venzke 1999; Inui 1997; Liu 1999; Miller et al. 1994) are therefore needed to investigate fully the dynamics, forcing, and possible feedbacks with the atmosphere of these thermal anomalies.

Acknowledgments. Discussions with Bruce Cornuelle, David Pierce, Tim Barnett, Paola Cessi, and Zhengyu Liu are gratefully acknowledged. The authors thank W. B. White for generously making available the subsurface temperature analysis. This work was supported by the National Science Foundation (NSF OCE97-11265), by the National Oceanic and Atmospheric Administration as part of the Experimental Climate Prediction Center (NA77RJ0453), and the Consortium for the Ocean's Role in Climate (NA47GP0188).

REFERENCES

Alexander, M. A., 1992: Midlatitude atmosphere–ocean interaction during El Niño. Part I: The North Pacific Ocean. *J. Climate,* **5,** 944–958.

Bjerknes, J., 1966: A possible response to the atmospheric Hadley circulation to equatorial anomalies of temperature. *Tellus,* **18,** 820–829.

Cayan, D. R., 1992a: Variability of latent and sensible heat fluxes estimated using bulk formulae. *Atmos.–Ocean,* **30,** 1–42.

——, 1992b: Latent and sensible heat flux anomalies over the northern oceans: Driving the sea surface temperature. *J. Phys. Oceanogr.,* **22,** 859–881.

Cushman-Roisin, B., 1987: Subduction. *Dynamics of the Oceanic Surface Mixed Layer: Proc. Aha Huliko: A Hawaiian Winter Workshop,* P. Muller and D. Henderson, Eds., Hawaii Institute of Geophysics, 181–196.

Da Silva, A. M., C. C. Young, and S. Levitus, 1994: *Atlas of Surface Marine Data 1994.* Vol. 1, *Algorithms and Procedures: NOAA Atlas NESDIS 6,* NOAA/NESDIS, 83 pp.

Deser, C. M., A. Alexander, and M. S. Timlin, 1996: Upper-ocean thermal variations in the North Pacific during 1970–1991. *J. Climate,* **9,** 1840–1855.

——, ——, and ——, 1999: Evidence for a wind-driven intensification of the Kuroshio Extension from the 1970s to the 1980s. *J. Climate,* **12,** 1697–1706.

Frankignoul, C., 1985: Sea surface temperature anomalies, planetary waves and air–sea feedback in the middle latitudes. *Rev. Geophys.,* **23,** 357–390.

——, P. Muller, and E. Zorita, 1997: A simple model of the decadal response of the ocean to stochastic wind forcing. *J. Phys. Oceanogr.,* **27,** 1533–1546.

Gill, A. E., 1982: *Atmosphere–Ocean Dynamics.* Academic Press, 662 pp.

Goddard, L., and N. Graham, 1997: El Niño in the 1990s. *J. Geophys. Res.,* **102,** 10 423–10 436.

Graham, N. E., 1994: Decadal scale variability in the 1970's and 1980's: Observations and model results. *Climate Dyn.,* **10,** 135–162.

Gu, D. F., and S. G. H. Philander, 1997: Interdecadal climate fluctuations that depend on exchanges between the Tropics and extratropics. *Science,* **275,** 805–807.

Inui, T., 1997: A numerical investigation of effects of westerlies variability on the circulation of subducted water. Ph.D. dissertation, Hokkaido University, Sapporo, Japan, 120 pp.

——, and K. Hanawa, 1997: A numerical investigation of effects of a tilt of the zero wind stress curl line on the subduction process. *J. Phys. Oceanogr.,* **27,** 897–908.

Jin, F. F., 1997: A theory of interdecadal climate variability of the North Pacific ocean–atmosphere system. *J. Climate,* **10,** 1821–1835.

Kleeman, R., R. A. Colman, N. R. Smith, and S. B. Power, 1996: A recent change in the mean state of the Pacific basin climate: Observational evidence and atmospheric and oceanic responses. *J. Geophys. Res.,* **101,** 20 483–20 499.

Latif, M., and T. Barnett, 1994: Causes of decadal climate variability over the North Pacific and North America. *Science,* **266,** 634–637.

——, and ——, 1996: Decadal climate variability over the North Pacific and North America: Dynamics and predictability. *J. Climate,* **9,** 2407–2423.

——, R. Kleeman, and C. Eckert, 1997: Greenhouse warming, decadal variability or El Niño? An attempt to understand the anomalous 1990s. *J. Climate,* **10,** 2221–2239.

Lau, N. C., 1997: Interactions between global SST anomalies and the midlatitude atmospheric circulation. *Bull. Amer. Meteor. Soc.,* **78,** 21–33.

Levitus, S., 1982: *Climatological Atlas of the World Ocean:* NOAA Prof. Paper 13, U.S. Govt. Printing Office, Washington, DC, 173 pp.

Liu, Z., 1996: Thermocline variability in different dynamical regimes. *J. Phys. Oceanogr.,* **26,** 1633–1645.

——, 1999a: Planetary waves in the thermocline: Non-doppler shift mode, advective mode and Green mode. *Quart. J. Roy. Meteor. Soc.,* in press.

——, 1999b: Forced planetary wave response in a thermocline gyre. *J. Phys. Oceanogr.,* **29,** 1036–1055.

——, and J. Pedlosky, 1994: Thermocline forced by annual and decadal surface temperature variations. *J. Phys. Oceanogr.,* **24,** 587–608.

Luyten, J. R., J. Pedlosky, and H. Stommel, 1983: The ventilated thermocline. *J. Phys. Oceanogr.,* **13,** 292–309.

Lysne, J., P. Chang, and B. Giese, 1997: Impact of the extratropical Pacific on equatorial variability. *Geophys. Res. Lett.,* **24,** 2589–2592.

Mantua, N. J., S. R. Hare, Y. Zhang, J. M. Wallace, and R. C. Francis, 1997: A Pacific interdecadal climate oscillation with impacts on salmon production. *Bull. Amer. Meteor. Soc.,* **78,** 1069–1079.

McCreary, J. P., and P. Lu, 1994: Interaction between the subtropical and equatorial ocean circulations: The subtropical cell. *J. Phys. Oceanogr.,* **24,** 466–497.

Miller, A. J., D. R. Cayan, T. P. Barnett, N. E. Graham, and J. M. Oberhuber, 1994a: The 1976–77 climate shift of the Pacific Ocean. *Oceanography,* **7,** 21–26.

——, ——, ——, ——, and ——, 1994b: Interdecadal variability of the Pacific Ocean: Model response to observed heat flux and wind stress anomalies. *Climate Dyn.,* **9,** 287–302.

——, W. B. White, and D. R. Cayan, 1997: North Pacific thermocline variations on ENSO time scales. *J. Phys. Oceanogr.,* **27,** 2023–2039.

——, D. R. Cayan, and W. B. White, 1998: A westward-intensified decadal change in the North Pacific thermocline and gyre-scale circulation. *J. Climate,* **11,** 3112–3127.

Pedlosky, J., 1983: Easter boundary ventilation and the structure of the thermocline. *J. Phys. Oceanogr.,* **13,** 2038–2044.

——, 1996: *Ocean Circulation Theory.* Springer-Verlag, 450 pp.

Philander, S. G. H., 1990: *El Nino, La Nina and the Southern Oscillation.* Academic Press, 293 pp.

Rayner, N. A., E. B. Horton, D. E. Parker, C. K. Folland, and R. B. Hackett, 1996: Version 2.2 of the global sea-ice and sea surface temperature data set, 1903–1994. Climate Research Tech. Note 74, 35 pp. [Available from Hadley Centre, London Rd., Bracknell, Berkshire RG12 2SY, United Kingdom.]

Robertson, A. W., 1996: Interdecadal variability over the North Pacific in a multi-century climate simulation. *Climate Dyn.,* **12,** 227–241.

Rothstein, L. M., R.-H. Zhang, A. J. Busalacchi, and D. Chen, 1998: A numerical simulation of the mean water pathways in the subtropical and tropical Pacific Ocean. *J. Phys. Oceanogr.,* **28,** 322–343.

Rhines, P. B., and W. R. Young, 1982: A theory of the wind-driven circulation. I. Midocean gyres. *J. Mar. Res.,* **40** (suppl.), 559–596.

Stommel, H., 1979: Determination of water mass properties of water pumped down from the Ekman layer to the geostrophic flow below. *Proc. Natl. Acad. Sci.,* **76,** 3051–3055.

Talley, L. D., 1985: Ventilation of the subtropical North Pacific: The shallow salinity minimum. *J. Phys. Oceanogr.,* **15,** 633–649.

——, 1988: Potential vorticity distribution in the North Pacific. *J. Phys. Oceanogr.,* **18,** 89–106.

Tourre, Y. M., Y. Kushnir, and W. B. White, 1999: Evolution of interdecadal variability in sea level pressure, sea surface temperature, and upper ocean temperature over the Pacific Ocean. *J. Phys. Oceanogr.,* in press.

Trenberth, K. E., 1990: Recent observed interdecadal climate changes in the Northern Hemisphere. *Bull. Amer. Meteor. Soc.,* **71,** 988–993.

——, 1991: Recent climate changes in the Northern Hemisphere. *Greenhouse-Gas-Induced Climate Change: A Critical Appraisal of Simulations and Observations,* M. E. Schlesinger, Ed., Elsevier, 377–390.

Venzke, S., 1999: Ocean–atmosphere interactions on decadal timescales. Ph.D. dissertation, University of Hamburg, 99 pp. [Available from Max-Planck-Institut für Meteorologie, Bundesstr. 55, D-20146 Hamburg, Germany.]

White, W. B., 1995: Design of a global observing system for gyre-scale upper ocean temperature variability. *Progress in Oceanography,* Vol. 36, Pergamon, 169–217.

Williams, R. G., M. A. Spall, and J. C. Marshall, 1995: Does Stommel's mixed layer ''Demon'' work? *J. Phys. Oceanogr.,* **25,** 3089–3102.

Yasuda, T., and K. Hanawa, 1997: Decadal changes in the mode waters in the midlatitude North Pacific. *J. Phys. Oceanogr.,* **27,** 858–870.

Zhang, R.-H., and S. Levitus, 1997: Structure and cycle of decadal variability of upper-ocean temperature in the North Pacific. *J. Climate,* **10,** 710–727.

——, L. M. Rothstein, and A. J. Busalacchi, 1998: Origin of upper-ocean warming and El Nino changes on decadal scales in the tropical Pacific Ocean. *Nature,* **391,** 879–883.